Int. J. Heat Mass Transfer. Vol. 10, pp. 1601–1613 Pergamon Press Ltd. 1967. Printed in Great Britain

RADIATION COUPLED SHOCK LAYER INCLUDING UPSTREAM ABSORPTION EFFECTS*

KUEI-YUAN CHIEN

Aerophysics Laboratory, Massachusetts Institute of Technology, Cambridge, Massachusetts

(*Received* 29 *August* 1966 *and in revised form* 31 *May* 1967)

Abstract—The method of Heaslet and Baldwin is extended with the introduction of a cold, black and porous wall, so as to effectively alter the downstream boundary condition for absorbing shock layers. It is shown that the general problem may be resolved into five subcases related to the net variation of radiative flux transfer across the shock with change in shock stand-off distance. The gas ahead of the shock may be either heated or cooled. For certain cases of interest this precursory heating may be significant.

NOMENCLATURE

$c_1, c_2,$ integration constants, equations (2) and (3), respectively;
$E_n,$ exponential integral of the nth order;
$F,$ defined by equation (20);
$G,$ defined by equation (22);
$h,$ enthalpy;
$K,$ radiation–convection parameter, below equation (13);
$K',$ reference K defined by equation (38);
$L,$ shock detachment thickness;
$l,$ upstream absorption length, equation (39);
$m,$ constant, equation (9);
$m_1,$ integration constant, equation (1);
$n,$ constant, equation (9);
$p,$ pressure;
$q,$ radiative flux;
$\bar{q},$ dimensionless radiative flux, equation (37);
$R,$ gas constant;
$T,$ temperature;
$\bar{T},$ dimensionless temperature, equation (36);
$u,$ velocity;
$v,$ normalized velocity, equation (11).

Greek symbols

$\gamma,$ gas constant;
$\theta,$ defined by equation (16);
$\theta_\infty,$ shock strength parameter, equation (17);
$\kappa,$ mass absorption coefficient;
$\xi,$ modified optical thickness, equation (10);
$\rho,$ density;
$\sigma,$ Stefan–Boltzmann constant;
$\tau,$ optical thickness (Bouguer number), equation (7);
$()_a, ()_b,$ ahead of and behind the shock, respectively;
$()_w,$ quantities evaluated at the wall;
$()^-, ()^+,$ immediately before and behind the shock, respectively.

* This work was supported by the Air Force Office of Scientific Research, Contract No. AF 49(638)-1621. Numerical results were obtained using the facilities of the Massachusetts Institute of Technology Computation Center. The author wishes to thank Professor J. R. Baron for his suggestions and discussions.

INTRODUCTION

THE PRESENCE of radiation as one of the mechanisms for energy transfer in a hypersonic flow complicates the problem considerably. Physically it eliminates the classical limitation to

downstream facing effects in supersonic flow. Mathematically it manifests itself by the appearance of a nonlinear integro-differential energy equation.

Yoshikawa and Chapman [1] considered the radiating shock layer problem assuming a non-absorbing upstream flow, the latter being included in a study of shock wave structures by Heaslet and Baldwin [2]. Of course, due to the inherent coupling between the upstream and downstream flow fields undergoing radiant energy exchanges across the shock, the shock layer cannot be treated independently. More precisely, all of the conditions, including temperature and local Mach number, for those points just ahead of the shock depend upon the body geometry, surface properties and far upstream fluid properties; consequently the conditions immediately behind the shock and the entire shock layer are affected in turn. In particular, the jump conditions across the inviscid shock discontinuity are unknown initially, and instead are to be found along with the shock wave "structure". Pai and Speth [3] have shown that the effective temperature jump across the shock is reduced by upstream heating in a shock structure problem, which can also be seen from the results shown in [2]. The introduction of a cold wall at a finite distance downstream makes possible both upstream cooling as well as heating, and it is the main interest of the present investigation to study the radiative flux coupling ahead and behind of a transparent inviscid shock discontinuity including the cold surface influence.

GOVERNING EQUATIONS

Some simplification of the rather complex general problem is appropriate. Consider the case of a uniform, hypersonic flow incident on a cold, black and porous wall. All properties in the flow field are assumed to be dependent on the single variable, x (see Fig. 1). For an inviscid, emitting and absorbing but otherwise perfect gas, in such a one-dimensional, steady flow, the governing equations are the familiar

$$\rho u = m_1 \tag{1}$$

$$p + m_1 u = m_1 c_1 \tag{2}$$

$$m_1(h + \tfrac{1}{2}u^2) - q = c_2 m_1 \tag{3}$$

$$p = \rho R T \tag{4}$$

$$h = \frac{\gamma}{\gamma - 1}\frac{p}{\rho}. \tag{5}$$

Here m_1, c_1 and c_2 are integration constants to be evaluated far upstream. Contributions from radiative pressure and radiative internal energy are assumed negligible, and the gas both grey and in local thermodynamic equilibrium. All notations in equations (1–5) are of standard form; the radiative flux term, q, is given by [4, 5]

$$q(\tau) = 2\sigma \int_{-\infty}^{\tau_w} \mathrm{Sgn}\,(t - \tau)\, T^4 E_2|t - \tau|\,\mathrm{d}t \tag{6}$$

and is defined to be positive in the negative x-direction. The optical thickness, τ, is defined as

$$\tau = \int_0^x \rho \kappa \,\mathrm{d}x \tag{7}$$

and attains its maximum positive value for the overall shock detachment thickness, L,

$$\tau_w = \int_0^L \rho\kappa \,\mathrm{d}x. \tag{8}$$

σ, E_2, and κ are the Stefan–Boltzmann constant, the exponential integral of the second order [4], and the mass absorption coefficient, respectively.

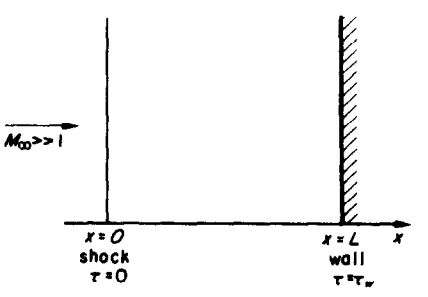

FIG 1. Schematic of flow.

The assumption of a porous wall results from the choice of a one-dimensional flow model and thus the need to absorb "mass". For hypersonic flow, the shock layer kinetic energy is much less than its thermal energy. Since our main interest is the determination of the thermal field, the introduction of a realistic cold wall as a heat sink is plausible. It is anticipated that a one-dimensional model will yield some useful insight into the behavior for multi-dimensional problems with the implied geometrical dilutation. It is worth noting that the one-dimensional model furnishes an upper-bound.

Since the differential approximation [6] method, or its equivalent kernel substitution method [7] in the one-dimensional case has been found to give rather accurate results for the shock structure problem [8], the same approximation has been adopted here. Hence we assume

$$E_2(\tau) \simeq m \exp(-n\tau). \tag{9}$$

Following Heaslet and Baldwin [2], we introduce a modified optical thickness parameter

$$\xi = n\tau \tag{10}$$

and a normalized velocity

$$v(\xi) = u(\tau)/c_1 \tag{11}$$

so that

$$T = \frac{c_1^2}{R} v(1 - v). \tag{12}$$

The governing equations can be combined into a single integral equation of the form

$$v^2 - \frac{2\gamma}{\gamma + 1} v + \frac{2(\gamma - 1)}{\gamma + 1} \frac{c_2}{c_1^2} = \frac{K}{8} \int_{-\infty}^{\xi_w} (v - v^2)^4 \operatorname{Sgn}(\xi - \xi_1) \exp(-|\xi - \xi_1|)\, d\xi_1 \tag{13}$$

where $K = 32m\sigma c_1^6(\gamma - 1)/(\gamma + 1)\, m_1 n R^4$, which is proportional to the ratio of the radiative to the convective energy transfer, i.e. an inverse modified Boltzmann number.

Far upstream ($\xi \to -\infty$) the right-hand side of equation (13) vanishes and $v = v_1$, say. If v_2 designates the other root for the case of vanishing q, then the left-hand side of equation (13) implies

$$v_1 + v_2 = \frac{2\gamma}{\gamma + 1}. \tag{14}$$

Since the radiative flux is continuous at the shock, where we set $\xi = 0$, equation (13) gives

$$v(0^-) + v(0^+) = \frac{2\gamma}{\gamma + 1} \tag{15}$$

where the superscripts + and − refer to immediately behind and before the shock, respectively. Of course, the radiation may modify $v(0^-)$ to something other than v_1. Thus the classical Rankine–Hugoniot conditions for conditions on the downstream side of a shock (and M_∞ free stream) are valid only when the net radiative flux at the shock vanishes.

For convenience introduce the continuous variable

$$\theta(\xi) = \left(\frac{\gamma}{\gamma + 1} - v\right)^2 = \theta_\infty + (v - v_1)(v - v_2) \tag{16}$$

where

$$\theta_\infty = \tfrac{1}{4}(v_1 - v_2)^2. \tag{17}$$

The point where the local Mach number is unity written in the present notation is given by

$$v^* = \frac{\gamma}{\gamma + 1} = \tfrac{1}{2}[v(0^-) + v(0^+)] \tag{17a}$$

and so we have

$$v(\xi) = \frac{\gamma}{\gamma + 1} - (\operatorname{Sgn}\xi)[\theta(\xi)]^{\frac{1}{2}}. \tag{18}$$

Consequently the governing equation can be recast as

$$\theta - \theta_\infty = \tfrac{1}{2} \int_{-\infty}^{\xi_w} \operatorname{Sgn}(\xi - \xi_1) F[\theta(\xi_1)] \exp(-|\xi - \xi_1|)\, d\xi_1 \tag{19}$$

where

$$F(\theta) = \frac{K}{4}\left[\frac{\gamma}{(\gamma+1)^2} + (\mathrm{Sgn}\,\xi)\left(\frac{\gamma-1}{\gamma+1}\right)\theta^{\frac{1}{2}} - \theta\right]^4. \tag{20}$$

Note that for a free stream Mach number approaching infinity, θ_∞ approaches $(\gamma+1)^{-2}$ (i.e. 0·1736 if $\gamma = \frac{7}{5}$).

Differentiating equation (19) with respect to ξ, we have

$$\frac{\mathrm{d}\theta}{\mathrm{d}\xi} = F - G \tag{21}$$

where

$$G = \tfrac{1}{2}\int_{-\infty}^{\xi_w} F(\theta[\xi_1])\exp(-|\xi - \xi_1|)\,\mathrm{d}\xi_1. \tag{22}$$

Thus

$$\frac{\mathrm{d}G}{\mathrm{d}\xi} = \theta_\infty - \theta \tag{23}$$

or finally

$$\frac{\mathrm{d}G}{\mathrm{d}\theta} = \frac{\theta_\infty - \theta}{F - G} \tag{24}$$

which is precisely the same relation developed by Heaslet and Baldwin [2] for the shock structure problem. Again both F and G have two branches, which will be denoted by subscripts a and b for ahead of and behind the shock, respectively.

The boundary conditions are

$$\xi \to -\infty: \quad \theta = \theta_\infty, \quad G_a = F_a(\theta_\infty) \tag{25}$$

$$\xi = \xi_w: \quad \theta = \theta(\xi_w) \equiv \theta_w, \quad G_b = \theta_w - \theta_\infty. \tag{26}$$

The far upstream boundary condition is identical to that for the shock structure problem, and follows upon combining equations (21) and (23) and noting that $(\mathrm{d}\theta/\mathrm{d}\xi)_{\xi\to-\infty} = 0$. The wall condition comes from equations (19) and (22). It will be clear that θ_w is a convenient starting value in place of the equivalent ξ_w.

The definition of G, equation (22), makes clear that G is a continuous function of ξ, and hence of θ. A solution may be obtained in the θ-plane by numerical integration of equation (24) from θ_∞ and θ_w for the respective branches, with equations (25) and (26) furnishing starting values. The shock exists at $G_a(\theta) = G_b(\theta)$ corresponding to $\xi = 0$. Equation (21) then implies $\xi = \xi(\theta)$ and a specific wall location, ξ_w, for the assumed θ_w.

SUBCASES

Physically the introduction of a cold wall introduces one more characteristic length, i.e. L. It also introduces the possibility of both upstream heating and cooling. In the limit as $\xi_w \to 0$, of course, the upstream temperature near the shock will decrease. As ξ_w increases, the temperature will increase until ξ_w is so large that the net radiative flux across the shock is zero. Of course, there will always be a radiative flux to the wall. As ξ_w increases still further, the net radiative flux across the shock faces upstream, and this, in turn, will increase the temperature immediately behind the shock. In the limit of an infinite shock layer thickness, far from the wall the effects of its presence should be negligible. This indicates a decoupling in the structure of the flow field, which consists of a shock structure tailed by an infinite subsonic stagnation flow over a cold wall.

Since positive ξ and x are in the same direction, the integrations starting from θ_∞ and θ_w, (i.e. from $\xi = -\infty$ and ξ_w) imply that $\mathrm{d}\xi_a > 0$ and $\mathrm{d}\xi_b < 0$, respectively. Equation (23) implies that $G_a(\theta)$ and $G_b(\theta)$ will go in the opposite direction for the same θ and the same sign of $\mathrm{d}\theta$.

Combining equations (21) and (24), we have

$$\frac{\mathrm{d}G}{\mathrm{d}\theta} = \frac{\mathrm{d}\xi}{\mathrm{d}\theta}(\theta_\infty - \theta) \tag{27}$$

which implies that

$$\frac{\mathrm{d}G_a}{\mathrm{d}\theta} < 0. \tag{28}$$

Since for the b-branch starting from $\theta_w < \theta_\infty$, $d\xi_b < 0$, and $\theta < \theta_\infty$, we have

$$\frac{dG_b}{d\theta} \lesseqgtr 0 \quad \text{for} \quad d\theta \gtreqless 0 \tag{29}$$

and G_a and G_b will never intersect when $\theta_w < \theta_\infty$. Consequently we have the relation

$$\theta_w > \theta_\infty. \tag{30}$$

Note that this implies that the velocity at wall will be always smaller than that without radiation and the assumption of a porous wall may be justified. This equation also implies that the wall temperature is lower than the corresponding radiationless case.

Also, equation (21) implies that

$$G_a \gtreqless F_a \quad \text{for} \quad \theta \lesseqgtr \theta_\infty \tag{31}$$

$$G_b < F_b \quad \text{for} \quad \theta < \theta_w. \tag{32}$$

Next, we wish to prove that G_a and G_b will not interesect at a point where $\theta > \theta_w$. If $\theta > \theta_w$ and $d\xi_b < 0$, $G_b > F_b$. Because of the fact that $F_b > F_a$,† equations (30) and (31) indicate that G_a and G_b will not intersect. Consequently we have

$$\theta < \theta_w. \tag{33}$$

Note that equation (33) combined with equation (18) imply that velocity is always decreasing in the shock layer from the shock toward the wall. Consequently for hypersonic flow the temperature in the shock layer is also monotonically decreasing from the shock to the wall.‡

From equation (33) it is clear that

$$\frac{dG_b}{d\theta} \lesseqgtr 0 \quad \text{for} \quad \theta \gtreqless \theta_\infty. \tag{34}$$

† This is true if $\theta < [\gamma/(\gamma+1)^2]$ but the equality implies $T_a < 0$ which is impossible.

‡ Equations (31) and (34) indicate that for the infinitely thick shock layer problem the largest θ_∞ which will allow G_a and G_b to intersect at the point $\theta = [(\gamma-1)/2(\gamma+1)]^2$ ($\equiv \theta_m$, say), which corresponds to a maximum F_b and $v(\theta_m) = \frac{1}{2}$, is $\theta_\infty = 9\theta_m$. For $\theta_\infty \geqslant 9\theta_m$ the temperature in the shock layer is monotonic. This θ_∞ corresponds to $M_\infty = 1{\cdot}89$ for $\gamma = 1{\cdot}4$. Clearly for a shock layer of finite thickness this condition is too strong.

From the above simple study of the G-function, we see clearly that all of the subcases mentioned earlier on the basis of physical arguments do exist. The various locii under discussion are shown in Fig. 2. Case 1 is the

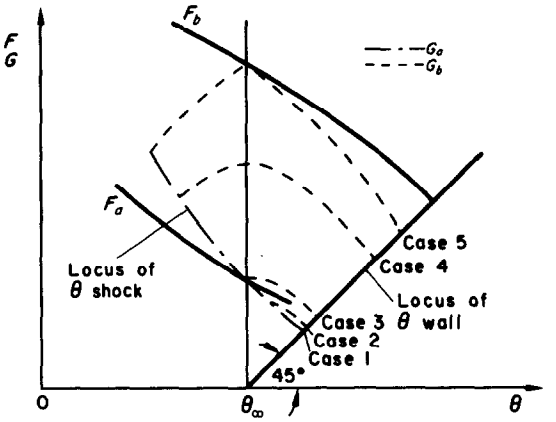

FIG. 2. Five subcases in F, G—θ plane.

limiting case of $\xi_w = 0$ ($\theta_{\text{shock}} = \theta_{\text{wall}}$). Case 3 separates those cases for which there is upstream heating (above) from those for cooling (below), which are represented as cases 4 and 2, respectively. Clearly case 3 corresponds to the classical uniform conditions of upstream flow and only in this special case do the classical Rankine–Hugoniot jump conditions across the shock (based on M_∞) remain valid. As ξ_w approaches infinity, the decoupling case arises (case 5).

The four parameters which characterize the problem are the free stream Mach number M_∞ (or θ_∞), the parameter indicating the relative importance of radiative to convective flux K (which is inversely proportional to the Boltzmann number), the specific heat ratio γ, and the modified optical thickness of the shock layer ξ_w. It is always possible to consider approximately the limiting cases analytically, e.g. small and large K [2]. But the main interest lies in the using of x_w instead of ξ_w as one of the parameters, which may answer the importance of radiation in the physical plane.

This proves to be somewhat complicated without using numerical integration.

Transformation from the ξ-plane to the x-plane requires some knowledge of the volumetric absorption coefficient, which was approximated by Shwartz [9] as

$$\frac{\rho\kappa}{(\rho\kappa)_0} \cong \frac{\rho}{\rho_0}\left(\frac{T}{T_0}\right)^5 \tag{35}$$

for air in the temperature range of 10^3–10^4 °K. The subscript zero refers to certain reference conditions, which were chosen to be $(\rho\kappa)_0 = 39{\cdot}3$ (ft^{-1}) at $T_0 = 32400°\text{R}$ and $\rho_0 = \rho_{\text{sea level}}$ [10]. We also choose $m = 1$ and $n = 1{\cdot}732$ (differential approximation [6]) which are required to evaluate x [see equation (9)].

RESULTS AND DISCUSSIONS

The importance of one of our four major parameters, namely, ξ_w, is apparent from Fig. 2. The range $0 \leqslant \xi_w \leqslant \infty$ corresponds to $1 \leqslant$ case number $\leqslant 5$. It is clear from Fig. 2 and equation (18) that the velocity upstream of the shock is accelerated for cases 1 and 2, decelerates for cases 4 and 5, and remains unchanged for case 3. The downstream velocity always decreases from the shock toward the wall as mentioned before. Velocity, and hence temperature if $\theta_\infty \geqslant 9\theta_m$, decreases at the wall and increases at the shock as ξ_w increases. The radiative flux, (defined positive in the negative x-direction), is always negative at the wall but there increases in magnitude as the shock layer thickens, but increases from a negative to a positive value at the shock. The flux at the shock vanishes for case 3, the value of ξ_w for which, ξ_{w_3} say, is a function of M_∞, K and γ. It is interesting to note that the radiative flux is monotonic as a function of ξ_w both at the shock and at the wall whereas Yoshikawa and Chapman [1] show some local maximum for certain cases at the wall. Because they used real gas tables and neglected upstream absorption, as compared with the present investigation, their problem has been reworked with a perfect gas model and somewhat different method [11], and a similar local maximum was found.

Equation (24) has been integrated numerically subject to equations (25) and (26). A dimension-

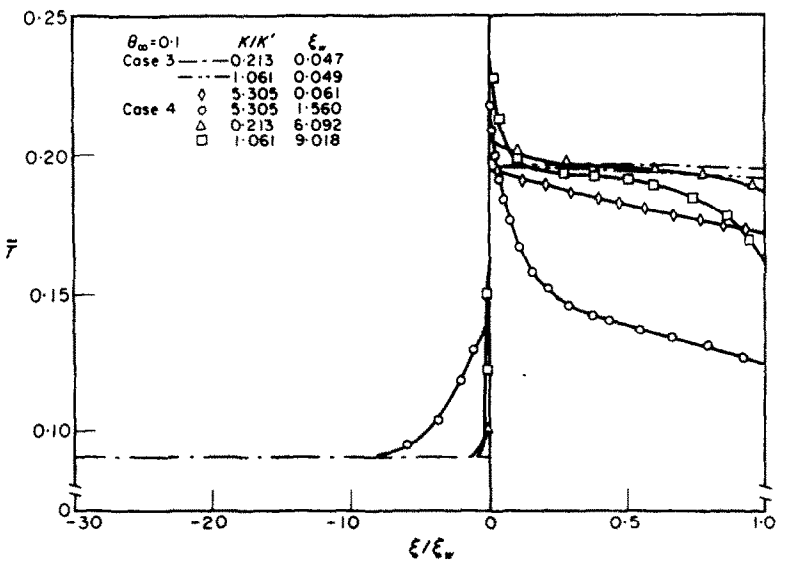

FIG. 3. Dimensionless temperature profiles.

less temperature $\bar{T}$ and a dimensionless radiative flux $\bar{q}$ have been defined as

$$\bar{T} \equiv \frac{RT}{c_1^2} = v - v^2 \tag{36}$$

$$\bar{q} \equiv \frac{2}{m_1 c_1^2}\left(\frac{\gamma - 1}{\gamma + 1}\right)\frac{q}{\theta_\infty} = \frac{\theta_\infty - \theta}{\theta_\infty}. \tag{37}$$

Note that $\bar{q}$ has been normalized by the strength of the shock, θ_∞, and hence relative magnitudes of $\bar{q}$ are comparable only for the same θ_∞. A constant

$$K' = 2(\sqrt{2})(\gamma + 1)^7\,\theta_\infty^{\frac{1}{2}}/\gamma^3(\gamma - 1) \tag{38}$$

was introduced by Heaslet and Baldwin [2] as a criterion for the relative importance of radiation for the shock *structure* problem, but it is not the sole criterion in the shock *layer* problem, as can be seen clearly in Fig. 3. It is also interesting to note (in Fig. 3) that a much stronger radiation effect exists near the shock for a relatively thick gas in the shock layer, in contrast to the same order effect both near the shock and the wall in [1]. Because of the possibility of both upstream heating and cooling as a function of all four parameters, or more precisely the fact that $\xi_{w_3} = \xi_{w_3}(K, \theta_\infty, \gamma)$, it is clear that $\xi_w K$ is *not* a universal scaling parameter for the thin gas limit. Fortunately the shock stand-off distance for case 3 (i.e. ξ_{w_3} or x_{w_3} in the ξ or x planes) has been found to be a weak function of K, depending instead rather strongly on θ_∞. Also, as shown in Table 1, the maximum upstream cooling effects are small enough, and decrease as θ_∞ increases, that for the case of interest to us, say $M_\infty \geqslant 10$, both x_{w_3} and ξ_{w_3} are small and only case 4 need be considered for practical purposes. It does result that $(\xi_w K/K')$ is an approximate scaling parameter for a thin gas for case 4. Local Mach number at the shock, $\bar{q}_w$ and $\bar{q}_s$, and wall temperature normalized with respect to the free stream temperature are shown in Figs. 4–6. In general the radiative effect is proportional to ξ_w/ξ_{w_3}, K/K' but inversely

Table 1. Dimensionless wall temperature and radiative flux at wall (shock) for case 1

θ_∞	K/K'	$T(0^-)/T(-\infty)$	$\bar{q}_w$
0·1	0·213	0·9909	−0·0065
0·1	1·061	0·9579	−0·0301
0·1	5·305	0·8477	−0·1095
0·13	0·213	0·9980	−0·00065
0·13	1·061	0·9899	−0·00335
0·13	5·305	0·9534	−0·01544

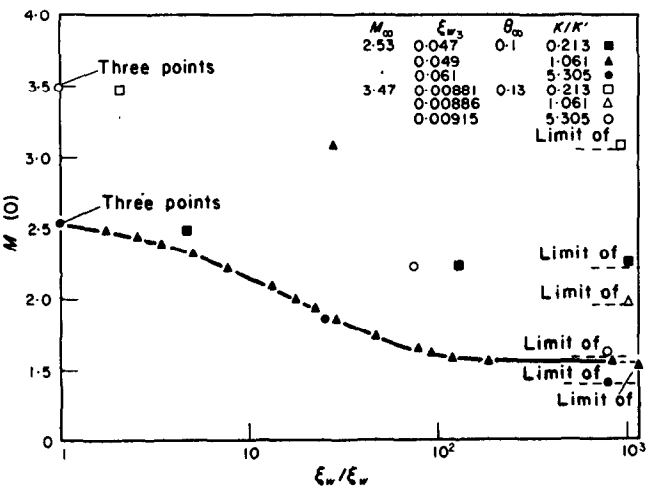

FIG. 4. Local Mach number at the shock.

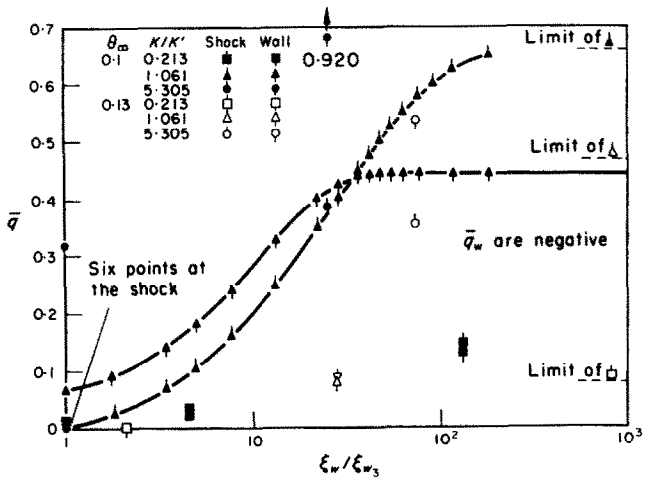

FIG. 5. Dimensionless radiative flux.

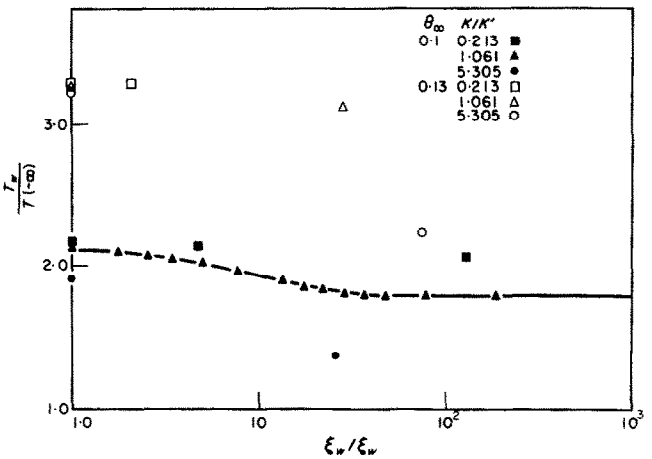

FIG. 6. Normalized wall temperature.

proportional to θ_∞. Note also that the local Mach number at the shock equals to the free stream Mach number when $\xi_w = \xi_{w_3}$. Three specific cases have been considered based on the atmospherical model of Minzner *et al.* [12]. They are tabulated in Table 2. Because of the lower density at higher altitudes, K may become very large for not too high Mach number. Since the volumetric absorption coefficient depends strongly on the temperature, and the latter depends heavily on the Mach number, especially in hypersonic flow, θ_∞ actually is a stronger parameter for the same x_w to

Table 2. θ_∞ and K/K'

Altitude (K ft)	M_∞	θ_∞	K/K'
100	10	0·16775	0·897
150	10	0·16775	12·592
100	15	0·17098	6·527

determine the radiative effects than K/K', as can be seen from Figs. 7–9; but K/K' is stronger for the same ξ_w, as shown in Fig. 10. It is clear from Fig. 7 that a shock layer of order one foot is not optically thin, especially at the high M_∞ cases of interest. In Fig. 10 also is shown $\bar{q}_w$ for one case as calculated without upstream absorption [11]. We can see a little hump there in contrast with the monotonic behavior obtained in the present investigation. There is also quite a difference in the asymptotic value of $\bar{q}_w$ for large Bouguer number. The inclusion of upstream absorption raises the temperature in the shock layer, and hence an increase of flux going into the wall. For low Bouguer number, the rise in temperature is small and so the effect is not

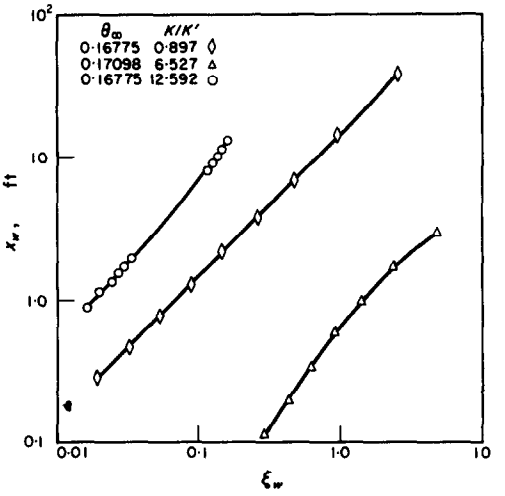

FIG. 7. Shock stand-off distance.

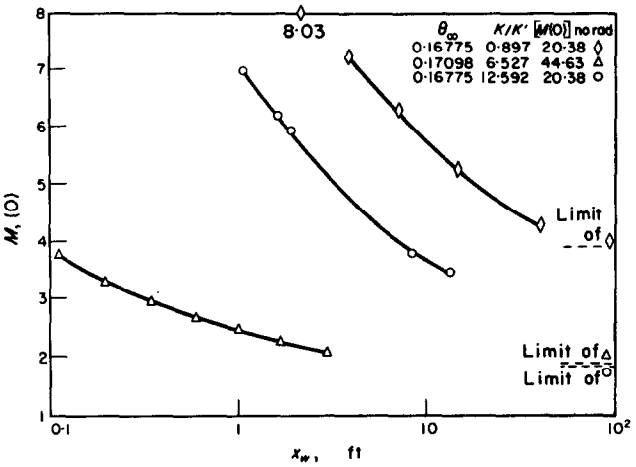

FIG. 8. Local Mach number at the shock.

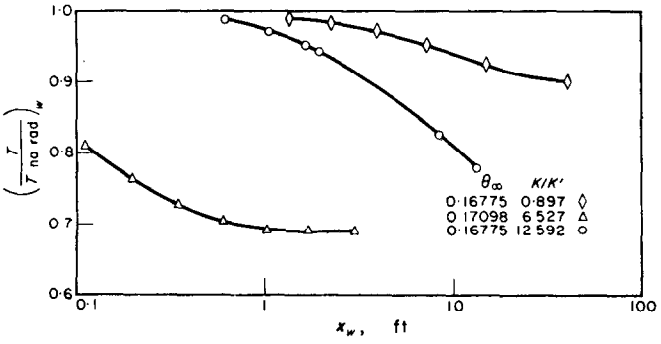

FIG. 9. Normalized wall temperature.

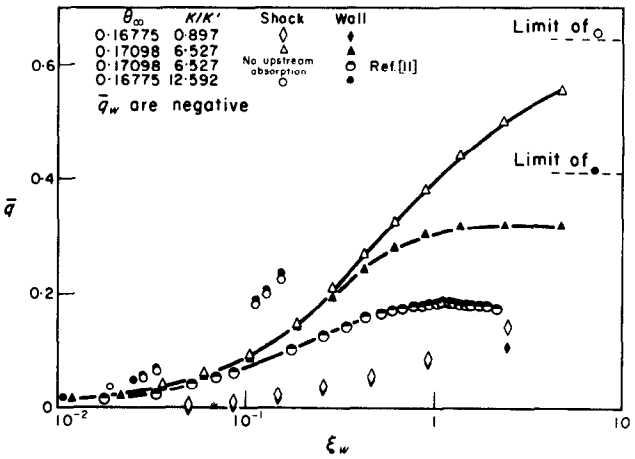

FIG. 10. Dimensionless radiative transfer.

pronounced. Without upstream absorption, the temperature right behind the shock is fixed for all Bouguer numbers with the same free stream Mach number. As the layer gets thicker, the temperature of the gas adjacent to the wall decreases [1]. This will decrease the "effective" temperature in the shock layer, and so it is plausible to find a local maximum. Temperature profiles are shown in Figs. 11 and 12, both in x and ξ coordinates.

Clearly the upstream heating effect is seen to be quite large, both in magnitude at the shock, and the range of its influence. This is similar to that in [2] where similar high temperature distribution relative to that of the free stream prevails for a length of the order of one photon mean free path. For atmospheric entry, this corresponds to a length of astronomical scale in the physical plane, simply because the volumetric absorption coefficient is temperature dependent and the atmospheric temperature is quite low. Of course, equation (35) is an approximation and spectral considerations would lead to strong absorption at relatively cold temperature levels in some bandwidths.

Define a characteristic upstream absorption length l by

$$\frac{T(0^-) - T(l)}{T(0^-) - T(-\infty)} = 0{\cdot}99 \qquad (39)$$

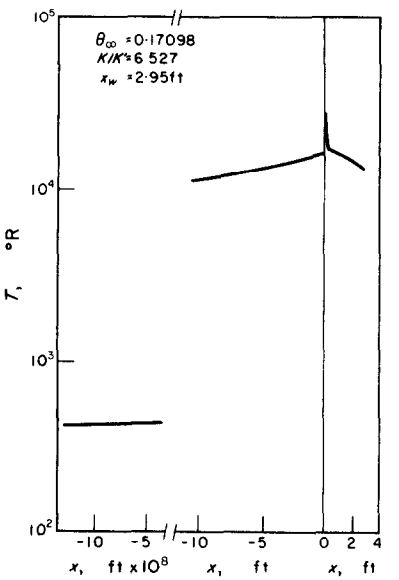

FIG. 11(a). Temperature profile.

For high free stream Mach numbers M_∞, $T(0^-) \cong T_t$, where T_t is the free stream stagnation temperature; since for air $T_t \cong M_\infty^2/5\ T(-\infty)$ we obtain

$$T(l) \cong 2 \times 10^{-3} M_\infty^2\ T(-\infty). \qquad (40)$$

Clearly for large M_∞, $T(l)$ may be high enough to give not too large an l. For example, with

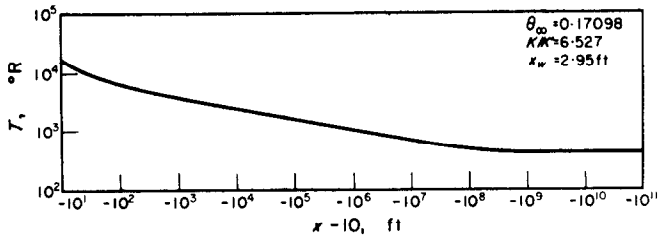

FIG. 11(b). Upstream temperature profile.

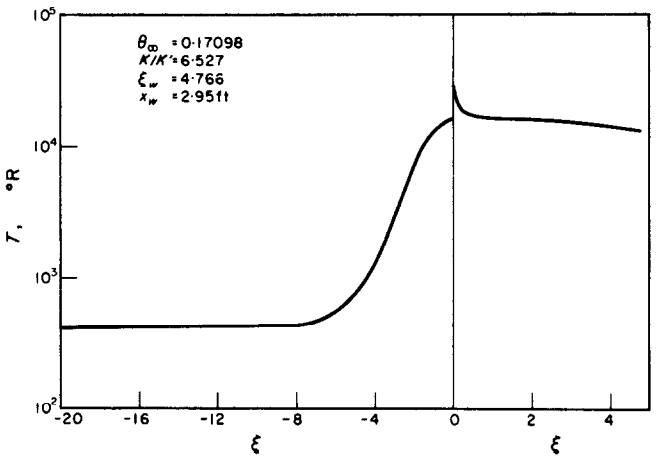

FIG. 11(c). Temperature profile.

$M_\infty = 50$ and $T(-\infty) = 4 \times 10^2\,^\circ R$, we obtain $l \cong 0$ (10^4) ft from Fig. 12(b). In the three-dimensional case, the energy flux in the steady state will be dilutated as $1/R^2$, where R is the distance from the body; we then expect $l \cong 0$ (10^2) ft. It is clear that equation (40) is valid only when $2 \times 10^{-3}\, M_\infty^2 \geqslant 1$.

In conclusion, it is of interest to compare the present results with those of [1, 2]. In the shock structure problem [2] radiation is directed upstream at the shock and vanishes somewhere far downstream, in contrast to the possible sign reversal within an actual shock layer. Similarly, from the same study, one may see that both $T(0^-)$ and $T(0^+)$, as well as T at any effective wall location, are larger than those for a finite shock layer. Since [1] neglects upstream absorption entirely, the isothermal oncoming stream implies underestimating both $T(0^-)$ and $T(0^+)$. Figure 10 shows the specific differences in flux magnitude and distribution in the two cases with and without upstream absorption under otherwise analogous conditions.

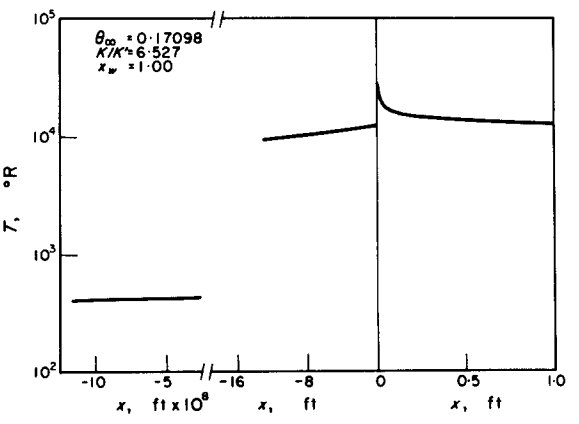

FIG. 12(a). Temperature profile.

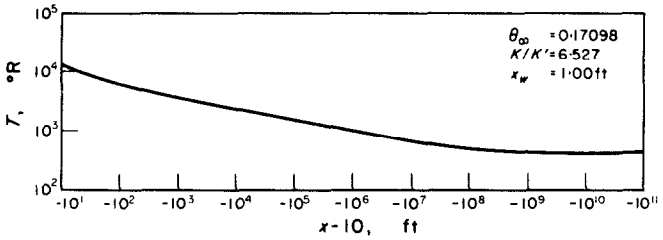

FIG. 12(b). Upstream temperature profile.

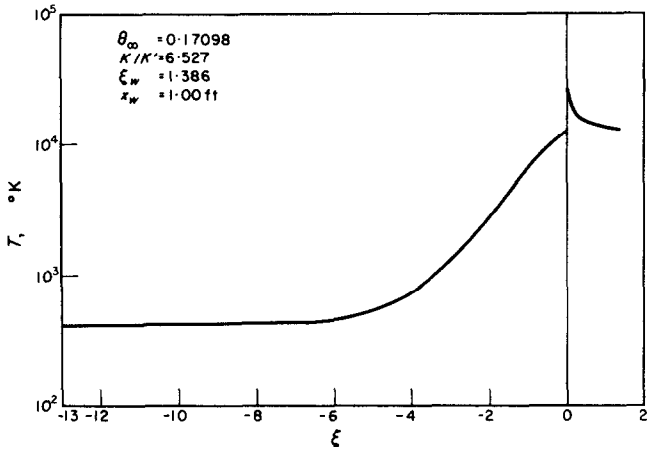

FIG. 12(c). Temperature profile.

REFERENCES

1. K. K. YOSHIKAWA and D. R. CHAPMAN, Radiative heat transfer and absorption behind a hypersonic normal shock wave, NASA TN D-1424 (1962).
2. M. A. HEASLET and B. S. BALDWIN, Predictions of the structure of radiation-resisted shock waves, *Physics Fluids* **6**, 781–791 (1963).
3. S. I. PAI and A. I. SPETH, Shock waves in radiation-magneto-gas dynamics, *Physics Fluids* **4**, 1232–1237 (1961).
4. V. KOURGANOFF, *Basic Methods in Transfer Problems*. Dover, New York (1963).
5. R. GOULARD and M. GOULARD, One dimensional energy transfer in radiant media, *Int. J. Heat Mass Transfer* **1**, 81–91 (1960).
6. P. CHENG, Two-dimensional radiating gas flow by a moment method, *AIAA Jl* **2**, 1662–1664 (1964).
7. W. G. VINCENTI and B. S. BALDWIN, Effect of thermal radiation on the propagation of plane acoustic waves, *J. Fluid Mech.* **12**, 449–477 (1962).
8. W. E. PEARSON, On the direct solution of the governing equation for radiation-resisted shock waves, NASA TN D-2128, 1964.
9. J. SHWARTZ, Radiation effects in the stagnation boundary layer, M.I.T. Aerophysics Lab. TR 119 (1965).
10. B. KIVEL and K. BAILEY, Tables of radiation from high temperature air, AVCO Res. Rept. 21 (December 1957).
11. M. C. JISCHKE, M.I.T. Aerophysics Lab., Private communication.
12. R. A. MINZNER, K. S. W. CHAMPTION and H. L. POND, The ARDC model atmosphere, 1959, AFCRC—TR-59-267 (August 1959).

Résumé—La méthode de Heaslet et Baldwin est étendue en introduisant une paroi poreuse, noire et froide afin de changer effectivement la condition à la limite aval pour l'absorption des couches de choc. On montre que le problème général peut être décomposé en cinq subdivisions reliées à la variation nette du transport par rayonnement à travers le choc avec un changement de la distance de détachement du choc. Le gaz en avant du choc peut être soit chauffé, soit refroidi. Dans certains cas intéressants, ce chauffage préliminaire peut être important.

Zusammenfassung—Die Methode von Heaslet-Baldwin wurde mit der Einführung einer kalten, schwarzen und porösen Wand erweitert, um die Grenzbedingungen für strombwärts gelegene, absorbierende Stoss-Schichten wirkungsvoll zu ändern. Es wird gezeigt, dass das Gesamtproblem in fünf Teilprobleme aufgelöst werden kann, die eine Beziehung herstellen zur Änderung des Strahlungswärmeflusses über die Stossfront bei Änderungen der Stosslage. Das Gas vor dem Stoss kann entweder erwärmt oder gekühlt sein. Für bestimmte Fälle kann diese vorhergehende Heizung von Bedeutung sein.

Аннотация—Метод Хисле и Болдуина был расширен посредством введения холодной, черной и пористой стенки для того, чтобы эффективно изменять граничное условие вниз по потоку для поглощающих ударных слоев. Показано, что общую задачу можно свести к пяти случаям, относящихся к изменению переноса лучистого потока поперек ударной волны с изменением расстояния от отошедшей ударной волны. Газ до скачка уплотнения может быть нагретым или холодным. В некоторых представляющих интерес случаях этот нагрев может быть значительным.